# HIGH-POWER PINCHED-BEAM DIODE DEVELOPMENT FOR RADIOGRAPHIC APPLICATIONS*

**David Hinshelwood[ξ], R.J. Allen, R.J. Commisso, G. Cooperstein, B.M. Huhman, S. L. Jackson, D. Mosher,[a] D.P. Murphy, P.F. Ottinger, J.W. Schumer, S.B. Swanekamp,[a] B.V. Weber, and F.C. Young[a]**

*Pulsed Power Physics Branch, Plasma Physics Division, Naval Research Laboratory*

*Washington, DC 20375 USA*

**J. Threadgold**

*AWE Aldermaston, UK*

**B. V. Oliver**

*Sandia National Laboratories*

*Abstract*

The negative-polarity rod-pinch diode has been studied at the 6-MV, 150-kA level on the NRL Mercury generator, in both reentrant and non-reentrant geometries. We observe good electrical coupling in reentrant geometry and satisfactory coupling in the non-reentrant case. In contrast to previous results at lower voltage, we see good electrical coupling to thin-walled aluminum anodes We see evidence that the diode geometry away from the rod tip plays a role in diode performance. Our best results to date are 75 rads at 1 meter with a 1.8-mm-diam spot. A spot size as low as 1.3 mm has been obtained, though at lower dose. The measured dose rate agrees very well with that predicted from particle-in-cell/Monte-Carlo modeling. An initial look at plasma-filled operation indicates that this technique is applicable to high-impedance diodes.

## I. INTRODUCTION

We are pursuing the development of high-voltage (~6 to 10 MV), small-spot-size (~1 to 2-mm-diam) x-ray sources for flash radiographic applications [1, 2]. This work is performed in close collaboration with Sandia and AWE, and is directed toward two separate goals: 1000 rads at 1 meter with a 2-mm spot size (these metrics are defined in the following) and 100 rads with a ~1.5-mm spot size.

This paper reports on studies of the rod-pinch (RP) diode [3], comprising a small anode rod and an annular cathode. Electrons emitted from the cathode pinch to the rod tip, resulting (nominally) in an x-ray source size defined by the rod diameter. This diode operates at impedances of 30-50 Ohms, and has been studied at voltages ranging from 1 to 6 MV [1]. As originally designed, the rod pinch operates in positive polarity, with the anode protruding through the (grounded) cathode out toward the object to be radiographed. However, both experiments and theory [2] show that as the voltage increases beyond 2-3 MV, the radiation output plummets relative to that expected from voltage scaling. This occurs because the electrons impact the rod primarily in the backwards direction. As the voltage increases, the x-radiation becomes more forward-peaked (relative to the electron direction), and thus directed primarily back into the generator. Therefore, at voltages of interest here, the diode must be operated in negative polarity, with the rod pointing back into the cathode. This arrangement is complicated by the need to extract the radiation back out through the anode structure.

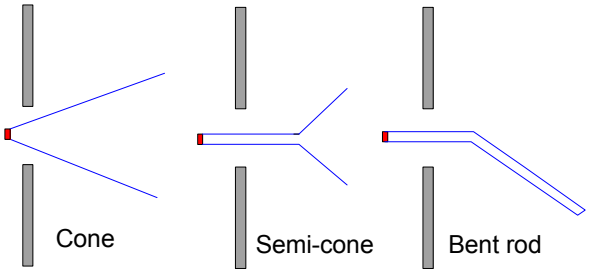


**Figure 1.** Extraction geometries for negative polarity.

Possible extraction geometries are sketched in Fig 1. We have *a priori* reservations about the cone geometry because of the fear of electron loss to the large-surface-area cone. In order to extract radiation efficiently using

* Work supported by the US Department of Energy through Sandia National Laboratories

ξ email: ddh@suzie.nrl.navy.mil

[a] L3-Titan, Reston, VA 20190 USA

# Report Documentation Page

*Form Approved*
*OMB No. 0704-0188*



| 1. REPORT DATE | 2. REPORT TYPE | 3. DATES COVERED |
|---|---|---|
| **JUN 2007** | **N/A** | **-** |

4. TITLE AND SUBTITLE
**High-Power Pinched-Beam Diode Development For Radiographic Applications**

5a. CONTRACT NUMBER
5b. GRANT NUMBER
5c. PROGRAM ELEMENT NUMBER

6. AUTHOR(S)

5d. PROJECT NUMBER
5e. TASK NUMBER
5f. WORK UNIT NUMBER

7. PERFORMING ORGANIZATION NAME(S) AND ADDRESS(ES)
**Pulsed Power Physics Branch, Plasma Physics Division, Naval Research Laboratory Washington, DC 20375 USA**

8. PERFORMING ORGANIZATION REPORT NUMBER

9. SPONSORING/MONITORING AGENCY NAME(S) AND ADDRESS(ES)

10. SPONSOR/MONITOR'S ACRONYM(S)
11. SPONSOR/MONITOR'S REPORT NUMBER(S)

12. DISTRIBUTION/AVAILABILITY STATEMENT
**Approved for public release, distribution unlimited**

13. SUPPLEMENTARY NOTES
**See also ADM002371. 2013 IEEE Pulsed Power Conference, Digest of Technical Papers 1976-2013, and Abstracts of the 2013 IEEE International Conference on Plasma Science. IEEE International Pulsed Power Conference (19th). Held in San Francisco, CA on 16-21 June 2013., The original document contains color images.**

14. ABSTRACT
**The negative-polarity rod-pinch diode has been studied at the 6-MV, 150-kA level on the NRL Mercury generator, in both reentrant and non-reentrant geometries. We observe good electrical coupling in reentrant geometry and satisfactory coupling in the non-reentrant case. In contrast to previous results at lower voltage, we see good electrical coupling to thin-walled aluminum anodes We see evidence that the diode geometry away from the rod tip plays a role in diode performance. Our best results to date are 75 rads at 1 meter with a 1.8-mmdiam spot. A spot size as low as 1.3 mm has been obtained, though at lower dose. The measured dose rate agrees very well with that predicted from particle-incell/ Monte-Carlo modeling. An initial look at plasmafilled operation indicates that this technique is applicable to high-impedance diodes.**

15. SUBJECT TERMS

| 16. SECURITY CLASSIFICATION OF: | | | 17. LIMITATION OF ABSTRACT | 18. NUMBER OF PAGES | 19a. NAME OF RESPONSIBLE PERSON |
|---|---|---|---|---|---|
| a. REPORT | b. ABSTRACT | c. THIS PAGE | | | |
| **unclassified** | **unclassified** | **unclassified** | **SAR** | **6** | |

the semi-cone or bent-rod schemes, the rod behind the tip should be as thin as possible.

Numerical simulations [2] predict an increasing ion current fraction as the voltage increases, reaching ~40% at 10 MV, and therefore reducing the x-ray output. The ion current can be reduced greatly by the use of a non-reentrant geometry, where the anode rod does not protrude through the cathode. For this geometry, the predicted x-ray dose matches that predicted for a more-conventional pinched-beam geometry. A non-reentrant geometry is also expected to increase the efficiency of radiation extraction, by reducing the length of the intervening rod, in the semi-cone and bent-rod arrangements. However, simulations also indicate that electrons are less likely to pinch efficiently to the tip of a non-reentrant rod at diode operating voltages below about 6 MV.

The (reentrant) negative-polarity rod pinch was studied extensively at the 4-5-MV level on the Sandia RITS-3 generator in 2004 [4]. Good electrical coupling to 2-mm-diam solid W rods was obtained, but the coupling was reduced when thin-walled Al rods were used. We report here on an extension to the RITS experiments, performed at the ~6-MV level on the NRL Mercury [5] generator. We have obtained good coupling to thin rods, demonstrating successful negative-polarity rod-pinch operation in realistic extraction geometries. We have also obtained reasonable coupling to non-reentrant rods.

## II. X-RAY DIAGNOSTICS

The x-ray dose is measured using $CaF_2$ thermoluminescent dosimeters (TLDs) enclosed in 1-cm-diam equilibrators and positioned in free space. All doses quoted here are in rads($CaF_2$) and normalized to a location 1 meter from the source. Additional filtration between the converter and TLD's arises from the rod material (and so varies for different configurations), a 1-cm-thick Al beamstop, and a 6-mm-thick Al vacuum flange.

The x-ray spot size is determined by interposing a tungsten rolled edge between the source and a radiographic-image-plate detector. Each point on the image records radiation from a half plane at the source. A line-out transverse to the edge is called the edge-spread function (ESF). The derivative of the ESF is termed the line-spread function (LSF). We use a dual-axis rolled edge, so that spot size can be determined along 2 axes.

Since the source distribution may have various functional forms, there is no unique metric of spot size. We use a modified version of the definition developed by AWE [6], where the spot is defined as 2.25 times the distance between the 25% and 75% points on the ESF. By reference, this corresponds to 90% of the diameter of uniform disk distribution, and 130% of the FWHM of a Gaussian distribution.

## III. EXPERIMENT

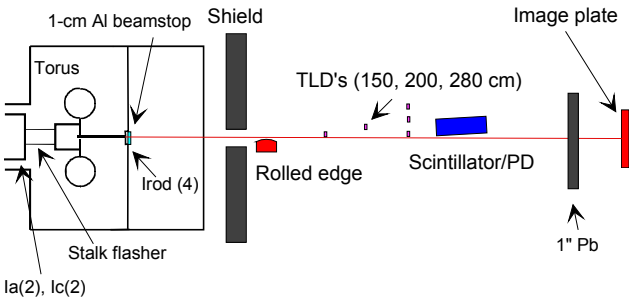


**Figure 2.** Experimental arrangement.

The experimental arrangement is shown in Fig. 2. Power flows into the diode region from the magnetically-insulated transmission line (MITL) of the 6-cavity inductive voltage adder. For the electrical parameters here, almost half of the generator current consists of electrons flowing in the MITL gap. To prevent these electrons from producing unwanted radiation (on the assumption that it is not possible to capture them at the rod tip), a toroidal structure at the end of the line acts to shed these electrons at large radius. An acrylic flashover switch located just before the torus reduces the diode prepulse to < 20 kV.

The diode current is determined from four dB/dt loops at the base of the anode. The voltage is calculated from the measured anode and cathode currents at the end of the MITL using magnetically-insulated flow theory [7, 8].

## IV. ELECTRICAL COUPLING

A series of shots diagnosed electrical coupling to the rod pinch. A 2-mm-diam, solid W rod was used on these shots. Because of the strong x-ray self absorption by the solid rod, the usual radiation diagnostics were less useful. The main diagnostics were the electrical waveforms and a side-viewing pinhole camera.

With the reentrant geometry, good coupling is obtained. Fig. 3 shows the reentrant geometry, the voltage, current, impedance, and photodiode signals, and a side-viewing pinhole photograph. The impedance is relatively flat at 40-45 Ohms. The voltage rise is slowed somewhat by the inductance of the long rod. The side-viewing pinhole image shows that the beam has pinched to the rod tip.

Next, we studied electrical coupling in the non-reentrant geometry. The diode was identical to that in Fig. 3, except that the rod was withdrawn so that its tip was located at 5, 10, and 20 mm from the front face of the cathode. Fig. 4 shows data from non-reentrant shots. The graph compares currents for non-reentrant shots with 5- and 10-mm axial gaps with those from the reentrant shot in Fig. 3. The currents shown are the diode current and the MITL anode current (which is indicative of the power pulse). At a 5-mm gap, the diode current rises as it does

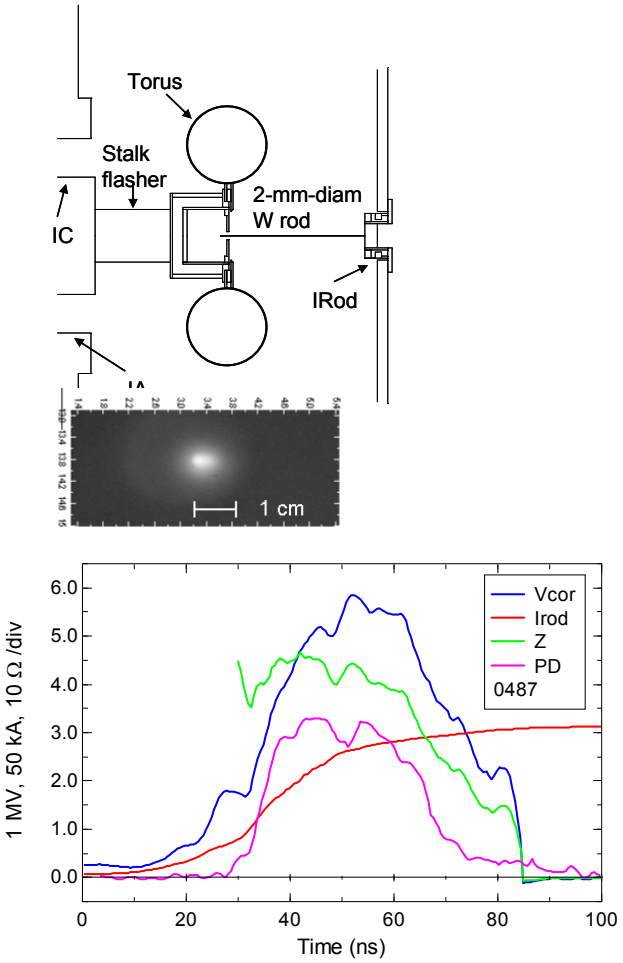


**Figure 3.** Reentrant rod pinch geometry, side-viewing pinhole photograph, and electrical data

in the re-entrant case, and the side-viewing x-ray pinhole image shows radiation concentrated at the tip. However, later in time the current rises sharply, indicative of impedance collapse. At a 10-mm gap, the impedance is stable, but the current rises slowly, and the x-ray image shows a distribution of radiation along the rod.

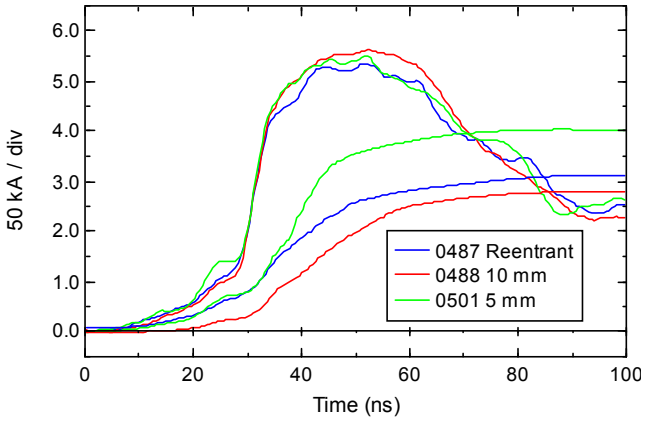


**Figure 4.** Currents from reentrant and non-reentrant shots.

We believe that with further optimization, we could achieve electrical coupling to the non-reentrant rod pinch approaching that achievable with the reentrant diode. This is consistent with simulation results indicating that the 6-MV voltage in this experiment is roughly the level at which the non-reentrant diode becomes feasible. These results suggest that the non-reentrant rod-pinch diode will be a very attractive option at still higher voltages.

Motivated by the results of earlier experiments at much lower voltage [9], the disk cathode was replaced by a cylinder as seen in the upper left of Fig 5. This shot exhibited a surprisingly rapid impedance collapse. Following this, a series of shots were taken with different geometries, both reentrant and non-reentrant, with a representative sample shown in Fig. 5. The results of this series indicated that coupling to the rod is degraded when the rod tip is located out from the torus rather than at the torus midplane. Faster collapse was seen for the disk cathode at the upper right, and even the reentrant geometry at the lower left. The recessed cylindrical-cathode geometry at the lower right, however, provided a stable impedance. Evidently, the overall diode geometry plays a role in electrical coupling. This is seen qualitatively in simulations using the particle-in-cell code LSP [10], pictured in Fig. 6. When the diode is out-thrust (right graph), the electrons flow mainly along the rod to the base. These results are significant in that they indicate that the overall diode geometry away from the rod plays a role in rod-pinch performance. We speculate that this is related to electrostatic focusing/defocusing early in time.

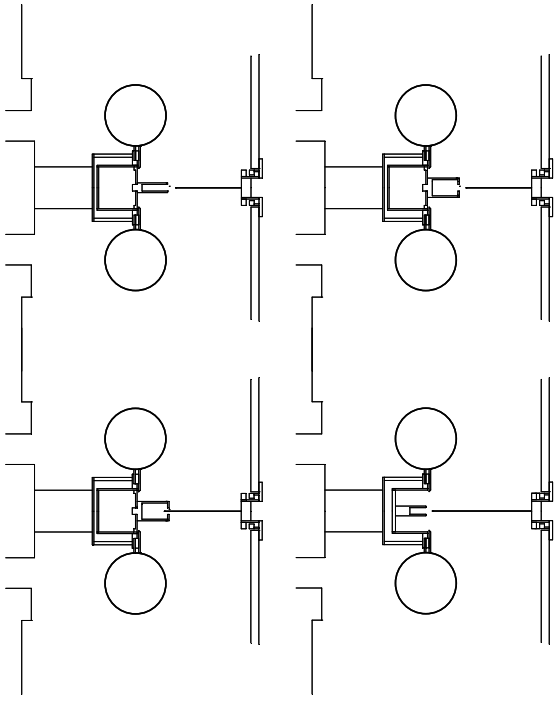

**Figure 5.** Different out-thrust and recessed geometries

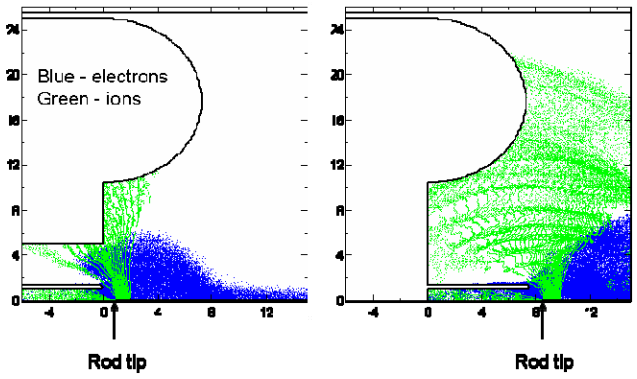


**Figure 6.** Particle plots from LSP simulations of out-thrust and recessed geometries.

## V. EXTRACTION GEOMETRIES

A series of shots were taken using a semi-cone geometry. Solid and hollow aluminum rods were used, with 3.5-to-5-mm-long gold or tungsten converters embedded in the tip. A sketch of the geometry is shown in Fig.7. The cone tip was located 6 cm from the cathode, and the rod tip was located at 1.6 cm beyond the cathode inner edge. The cone structure provided a 3-degree half-angle field of view, over which the absorption was limited to the ~8-cm-long rod. The cathode diameter was ten times the rod diameter.

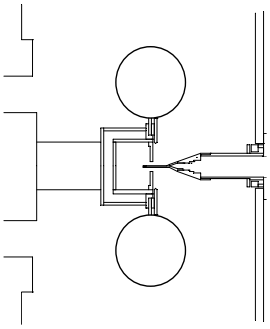

**Figure 7.** Semi-cone geometry.

Representative results are shown in Table 1. (At the thinnest wall thickness of 0.02 mm, a 2-cm-length of 0.9-mm-diam graphite was inserted in the tube behind the converter.) .

**Table 1.** Typical semi-cone results, listing the rod OD, wall thickness, converter diameter, and AWE spot (all in mm), with the dose in rads@1m.

| Shot | Rod | Wall | Dia | Dose | Spot |
|---|---|---|---|---|---|
| 0522 | 3 | 0.5 | 2 | 51 | 2.1 |
| 0523 | 3 | 0.7 | 1.6 | 46 | 1.8 |
| 0524 | 2.1 | 0.25 | 1.6 | 75 | 1.8 |
| 0527 | 1 | 0.02 | 1.0 | 31 | 1.3 |

These results represent a marked improvement over the lower-voltage RITS results, where poor coupling to aluminum rods was observed. Here, we see good coupling to wall thicknesses down to 0.25 mm.

Results for the best shot (0524) are shown in Fig.8. The impedance history is similar to that seen with a 2-mm-diam solid tungsten anode. With the aluminum anode, the early-time impedance is slightly higher, which is reflected in the slightly more slowly-rising radiation pulse. We speculate that this difference arises from slower ion turn-on with the aluminum anode than with the tungsten anode.

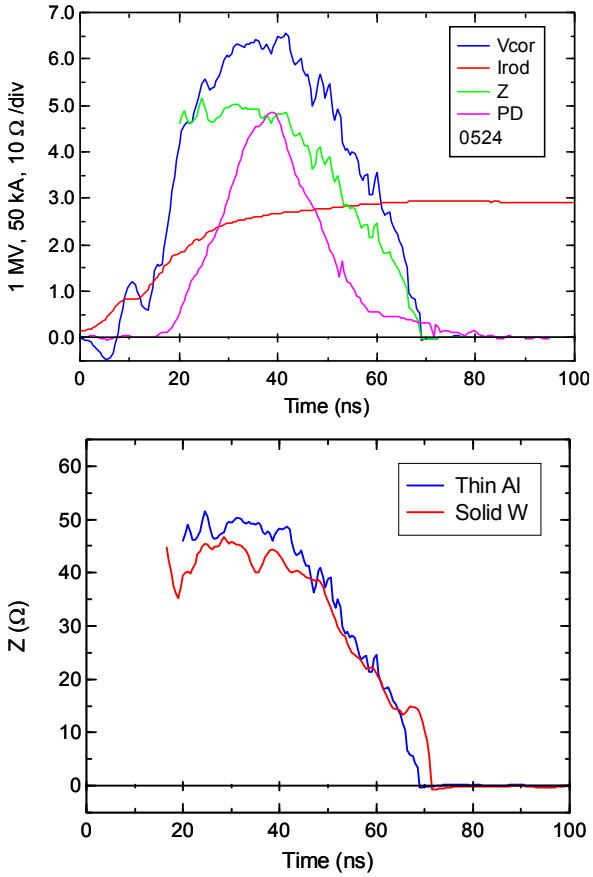


**Figure 8.** Electrical data for the shot from the third row in Table 1, and a comparison of its impedance history with that for a solid-W-rod shot.

Fig. 9 shows the measured line-spread functions for shots 0524 and 0527. Calculated line spreads for ideal disk sources are shown for comparison. The measured data are consistent with disk sources slightly larger than the converter diameter, along with moderate wings. These wings can arise either from radiation by material expanding from the rod tip or by electron deposition at the base of the rod. Future work will clarify the role played by each of these factors.

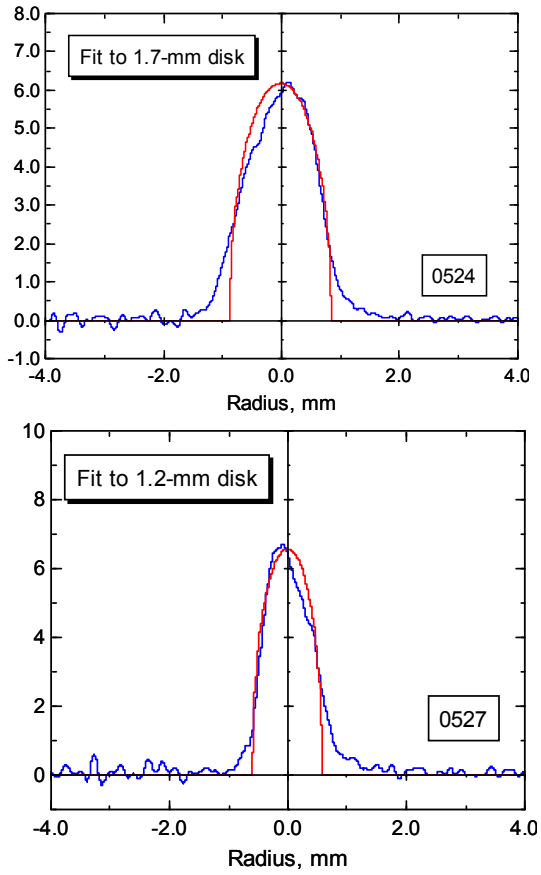


**Figure 9.** Measured line-spread functions for shots 0524 and 0527, compared with disk line-spread functions.

## VI. MODELING

Rod-pinch diode operation is modeled using LSP and the Sandia Monte-Carlo code ITS [11]. Typical results are shown in Fig. 10.

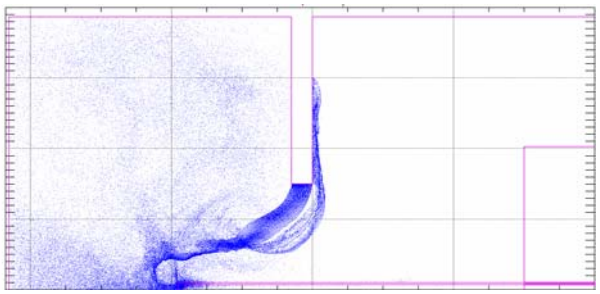

**Figure 10.** LSP Modeling of the rod-pinch diode.

LSP calculates the particle motion in the diode and the resulting photon production in the anode, while ITS follows the photons out through the anode structure. The TLD response is then determined analytically. A series of LSP runs at different voltages yields a predicted scaling of radiation dose rate with voltage. This is combined with the measured diode current and voltage to give a calculated dose rate. The measured dose rate is determined from the TLD yield and the photodiode signal. These two are compared in Fig 11, and excellent agreement is seen. (Note that this is an absolute comparison, without any normalization.)

Modeling also predicts a ~50% reduction in dose with the thinner, 1-mm-diam anodes, consistent with experiment (see Table 1). Examination of the model results shows that this decrease results from both an increase in the ion current fraction, and an increase in the average electron incidence angle (thus reducing the dose rate in the forward direction).

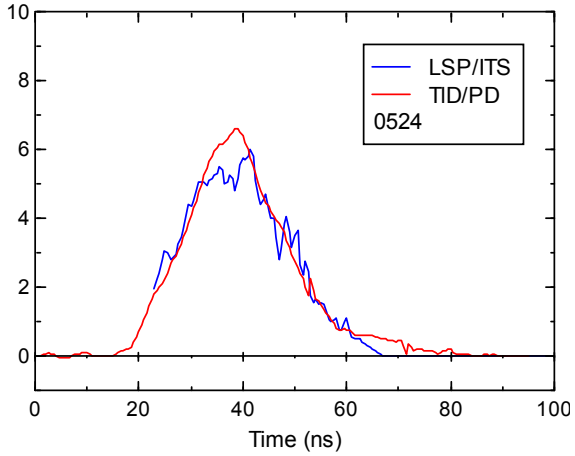


**Figure 11.** Comparison of calculated and measured x-ray dose rate.

## VII. PLASMA INJECTION

The plasma-filled rod pinch [12] operates at a few Ohms and produces exceptional x-ray source characteristics. We are investigating the application of plasma-fill techniques to high-impedance diodes. The hope is that a judicious use of pre-injected plasma may enhance pinch formation, improving the coupling efficiency and localizing the pinch. Possible injection techniques are shown in Fig. 12. For the reentrant pinch, plasma can be injected radially as in [12]. For the non-reentrant pinch, the use of a laser to ablate plasma from the tip appears attractive.

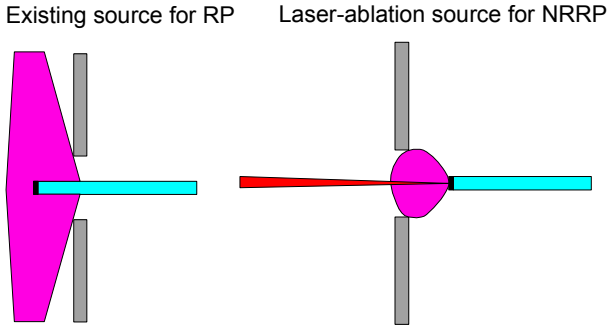


**Figure 12.** Plasma injection schemes.

We have constructed a plasma-gun surrogate for the laser ablation source: a coaxial plasma gun is built into a 2-mm-diameter rod. This source has been characterized using interferometry [13] and fielded on one shot. The cylindrical-cathode geometry of Fig. 5 (upper left) is used, since we know that coupling is poor in this case without plasma. The plasma density at the cathode is about 6 x $10^{14}$ cm $^{-3}$ at the time of the generator pulse. In this case, the diode begins as a short circuit before opening to a low impedance. Evidently the plasma density was too high. Nonetheless, we see classical plasma-filled diode behavior, and are optimistic about the prospects for an optimized source.

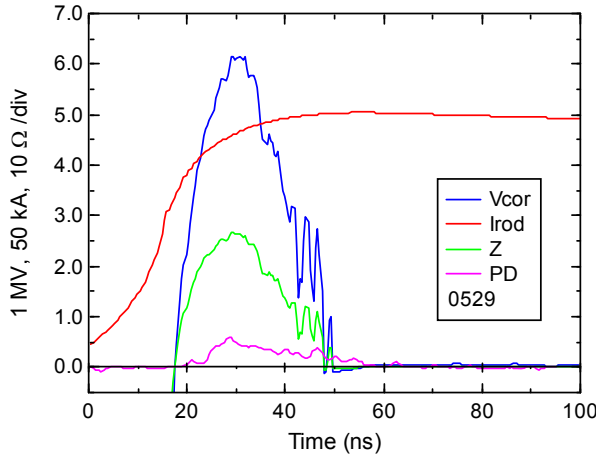


**Figure 13.** Results from an initial shot with plasma injection

## VIII. SUMMARY

The negative-polarity rod-pinch diode has been studied at the 6-MV, 150-kA level, in both reentrant and non-reentrant geometries. The electrical coupling obtained in the non-reentrant geometry indicates that this approach is viable at voltages > 6 MV. In reentrant geometry, we find good electrical coupling to thin-wall aluminum anodes, in contrast to previous results at lower voltage. We see evidence that the diode geometry away from the rod tip plays a role in diode performance. Our best results to date are 75 rads at 1 meter with a 1.8-mm diam spot. A spot size as low as 1.3 mm has been obtained, though at lower dose. The measured dose rate agrees very well with that predicted from modeling. An initial look at plasma-filled operation indicates that this technique is applicable to high-impedance diodes.

## IX. REFERENCES


[1] J. Maenchen, G. Cooperstein, J. O'Malley, and I. Smith, "Advances in Pulsed-Power-Driven Radiography Systems," *Proceeding of the IEEE* vol. 92, no. 7, pp. 1021-1042, July 2004.

[2] S.B. Swanekamp, et al., "An Evaluation of Self-Magnetically-Pinched Diodes for Voltages Up to 10 MV as High-Resolution Flash X-Ray Sources," *IEEE Trans. Plasma Sci.*, IEEE Trans. Plasma Sci. vol. 32, no. 5, pp. 2004-2016, Oct. 2004.

[3] G. Cooperstein, et al., "Theoretical modeling and experimental characterization of a rod-pinch diode", *Phys. Plasmas*, vol. 8, no. 10, pp. 4618-4636, Oct. 2001.

[4] G. Cooperstein, et al.,, "Negative-Polarity Rod-Pinch Diode Experiment at 5 MV on RITS-3," in the Proceedings of the 15th IEEE International Pulsed Power Conference, (Monterey, CA, June 2005), p. 851.

[5] R.J. Allen, et al., "Initialization and Operation of Mercury, a 6-MV MIVA (Magnetically-Insulated Inductive Voltage Adder)," in the Proceedings of the 15th IEEE International Pulsed Power Conference, (Monterey, CA, June 2005), pp. 338-342.

[6] T. J. Goldsack,et al., "Multimegavolt multiaxis high-resolution flash X-ray source development for a new hydrodynamics research facility at AWE Aldermaston," IEEE Trans. Plasma Sci., vol. 30, pp. 239-253, Feb. 2002.

[7] C.W. Mendel and S. E. Rosenthal, "Dynamic modeling of magnetically insulated transmission line systems," *Phys Plasmas* vol. 3, no. 11, pp. 4207-4219, Nov. 1996, and references therein.

[8] P. F. Ottinger and J. W. Schumer, "Rescaling of equilibrium magnetically insulated flow theory based on results from particle-in-cell simulations," *Phys. Plasmas* vol. 13, no. 6, TOC 063109, June 2006.

[9] G. Cooperstein, et al., "A High-Impedance, Ion-Enhanced, Electrostatically-Focused Diode for Flash Radiography," presented at the 16th International Conference on High-Power Particle Beams (Oxford, UK, July 2006).

[10] D.R. Welch, et al., "Simulation techniques for heavy ion fusion chamber transport ", *Nucl. Meth. Phys. Res. A,* vol. 464, no. 1-3. pp. 134-139, May 2001.

[11] J.A. Halbleib, et al., "ITS: The Integrated TIGER Series of electron/photon transport codes-Version 3.0*",* *IEEE Trans. Nucl. Sci.*, vol. 39, no. 4, pp 1025-1030, August, 1992.

[12] B. V. Weber, et al., "Plasma-Filled Rod-Pinch Diode Research on Gamble II," these proceedings, and references therein.

[13] S. L. Jackson, et al., "Electron Density Measurements on Radiographic Diodes," these proceedings.